

High-spin states in ^{35}S

S. Go^{1,2}, E. Ideguchi,³ R. Yokoyama,² N. Aoi,³ F. Azaiez,⁴ K. Furutaka,⁵ Y. Hatsukawa,⁵ A. Kimura,⁵ K. Kisamori,² M. Kobayashi,² F. Kitatani,⁵ M. Koizumi,⁵ H. Harada,⁵ I. Matea,⁴ S. Michimasa,² H. Miya,² S. Nakamura,⁵ M. Niikura,⁶ H. Nishibata,^{1,7} N. Shimizu,² S. Shimoura,² T. Shizuma,⁵ M. Sugawara,⁸ D. Suzuki,^{4,9} M. Takaki,² Y. Toh,⁵ Y. Utsuno,⁵ D. Verney,⁴ and A. Yagi⁷

¹Department of Physics, Kyushu University, 744 Motoooka, Fukuoka 819-0395, Japan

²Center for Nuclear Study, The University of Tokyo, 2-1 Hirosawa, Wako, Saitama 351-0106, Japan

³Research Center for Nuclear Physics, Osaka University, 10-1 Mihogaoka, Ibaraki, Osaka 567-0047, Japan

⁴Université Paris-Saclay, CNRS/IN2P3, IJCLab, 91405 Orsay, France


⁵Japan Atomic Energy Agency, 4-49 Muramatsu, Tokai, Naka, Ibaraki 319-1194, Japan

⁶Department of Physics, The University of Tokyo, 7-3-1 Hongo, Bunkyo-ku, Tokyo 113-0033, Japan

⁷Department of Physics, Osaka University, 1-1 Matikaneyamamati, Toyonaka, Osaka 560-0043, Japan

⁸Chiba Institute of Technology, 2-1-1 Shibazono, Narashino, Chiba 275-0023, Japan

⁹RIKEN Nishina Center, 2-1 Hirosawa, Wako, Saitama 351-0198, Japan

 (Received 11 November 2020; revised 29 November 2020; accepted 16 March 2021; published 29 March 2021)

Excited states in ^{35}S were investigated by in-beam γ -ray spectroscopy using the $^{26}\text{Mg}(^{18}\text{O}, 2\alpha n)$ fusion-evaporation reaction. The deexciting γ rays were measured with germanium detector arrays along with the measurement of evaporated charged particles in a 4π -segmented Si detector array. The level scheme was extended up to 12.47 MeV. The obtained level structure is compared with the large-scale shell-model calculations. The possibility of isoscalar-pair excited states is discussed for $J = (17/2)$ states with comparison between the experimental and theoretical results.

DOI: [10.1103/PhysRevC.103.034327](https://doi.org/10.1103/PhysRevC.103.034327)

I. INTRODUCTION

Nuclear properties, such as binding energies [1] and the spectroscopy of excited states [2] suggest that isovector ($T = 1$) proton-neutron (pn) pairing is dominant at low-excitation energies. On the other hand, isoscalar ($T = 0$) pn pairing is less clear and is often debated [3–5]. Recent noteworthy experimental works indicate the role of the interaction at low-spin states in $N = Z$ nuclei [6,7]. The isoscalar pn interaction plays an important role in the occurrence of the high-spin β -decaying 16^+ state in ^{96}Cd [8]. The isovector pairing correlations are supposed to be rapidly suppressed with increasing angular momentum, whereas the isoscalar pairing correlations relatively fall off at a slower rate [9–11]. The study on the pairing interactions has been focused mainly on the $N = Z$ nuclei. However, it could be extended to $N \neq Z$ nuclei. The promotion of the isoscalar pn pair to the fp shell was discussed at the high-spin states in ^{34}S [12]. Further experimental investigation is necessary to clarify such excitation. Here, we extended the study to the high-spin states in ^{35}S .

In addition to the pn correlation, interesting phenomena, such as emergence of superdeformed (SD) bands [13–15], clusterization in nuclei [16,17] can be studied in sd -shell nuclei. To describe the high-spin states in this region, cross-shell excitations from the sd to the fp shells have to be taken into account. The emergence of SD bands in ^{36}Ar [13], ^{40}Ar [14], and ^{40}Ca [15] is attributed to the multiparticle multihole excitations. The low-spin structure has been reproduced well

by shell-model calculations with, such as the universal sd (USD) interaction [18]. However, there are still considerable uncertainties in the high-spin states between experimental and theoretical results. Investigations on the high-spin states provide constraints and testing grounds for more recent effective interactions [19–23]. As for sulfur isotopes, cluster properties in ^{34}S were discussed in the low-spin states [24] whereas the promotion of the isoscalar pn pair was reported in the high-spin states [12]. The excited states of odd-mass nuclei $^{33,35}\text{S}$ [25,26] has been extensively studied with different effective interactions.

In this paper, we investigated high-spin states of ^{35}S by a fusion evaporation reaction of $^{26}\text{Mg}(^{18}\text{O}, 2\alpha n)$ to investigate the isoscalar pn -pair excitation. Prior to this paper, there is a significant body of experimental studies on the excited states, such as the β decay of ^{35}P [27], $^{34}\text{S}(n, \gamma)$ [28], $^{34}\text{S}(d, p\gamma)$ [29], $^{37}\text{Cl}(p, ^3\text{He})$ [30], $^{37}\text{Cl}(d, \alpha\gamma)$ [31], $^{24}\text{Mg}(^{14}\text{N}, 3p)$ [26], and transfer reaction of ^{37}Cl [32]. We extended the level scheme up to 12470 keV with $J = (21/2)$ from the previously known level at 8023 keV with $J^\pi = (17/2^+)$ [26]. The observed levels in this paper are compared with large-scale shell-model calculations including the sd - fp model space with the ^{16}O core. The high-spin structure of ^{35}S and the promotion of the isoscalar couplings in the high-spin states are discussed on the basis of the experimental and theoretical results.

This paper begins with a description of the experimental detail and results in Sec. II. A comparison of the experimental

data with large-scale shell-model calculations is described in Sec. III. The results of this paper are summarized in Sec. IV.

II. EXPERIMENTAL RESULTS

To investigate the high-spin states of ^{35}S , two experiments were conducted. The first experiment was performed at the JAEA tandem accelerator facility to determine the beam energy for producing high-spin states of ^{35}S . The heavy-ion fusion evaporation reaction of $^{26}\text{Mg}(^{18}\text{O}, 2\alpha 1n)^{35}\text{S}$ was used. The target consisted of a self-supporting metallic enriched foil of ^{26}Mg which has 0.5-mg/cm^2 thickness. The measurement of the γ rays was conducted with the germanium detector array GEMINI-II [33] with the BGO Compton suppressor shield. A total of 14 germanium detectors were placed with five different angles. The γ -ray energies measured in the laboratory frame were corrected for Doppler shifts by the velocity of the fusion residue of ^{35}S outside the target. The velocity was obtained by fitting peak positions of previously known γ -ray transitions [26] as a function of the detector angles. The beam energy of 80 MeV was selected by comparing the ratio of the high-spin to low-spin states of ^{35}S with different beam energies among a set of measurements at 70, 80, 95, and 110 MeV [34].

The second experiment to investigate high-spin states of ^{35}S was conducted at the ALTO-Tandem facility with the beam energy. In order to measure the γ -ray transitions from the high-spin states, the germanium detector array ORGAM based on the EUROGRAM [35] with the BGO scintillator for the anti-Compton suppressor, was employed. A total of 13 detectors was installed at four different angles at 47° , 86° , 94° , and 158° with respect to the incident ^{18}O beam.

The excited states of ^{35}S were populated via $2\alpha 1n$ evaporation from the compound nucleus of ^{44}Ca . The reaction channel was selected by measuring the evaporated charged particles with a 4π -silicon detector [36] in both experiments. The array consists of 170 μm -thick pentagonal-shape detectors. Each detector was arranged in a regular dodecahedron frame. The most forward silicon detector and the second forward detectors were segmented into five and two sections, respectively, to have a capability for the high-count rate of the evaporated charged particles. In order to avoid the scattered ^{18}O beam entering into the detector, thin aluminum absorbers were set in front of each detector. The thickness of the absorber was selected to be $8\text{-}\mu\text{m}$ thick with an additional gold foil of $15\text{ }\mu\text{m}$ for the most forward angle, 50 and $40\text{ }\mu\text{m}$ for the second forward and the backward angles, respectively. The overall efficiency for a single α particle was estimated to be 60% by comparing γ -ray intensities in the 1α - and 2α -gated γ -ray spectra of ^{35}S . The use of the multicharged particle gate significantly reduced the γ -ray background produced by different evaporation channels during the experiment.

To construct the level scheme, γ - γ coincidence analysis with the 2α detection in the Si detector array was performed. Spectra gated by the low-lying transitions are shown in Fig. 1. The gate on the 1991-keV transition shows the peaks related to the previously known transitions with the different reaction of $^{24}\text{Mg}(^{14}\text{N}, 3p)^{35}\text{S}$ [26]. The gate on the intense transition at 1302 keV revealed four new transitions of 732, 1576, 2421,

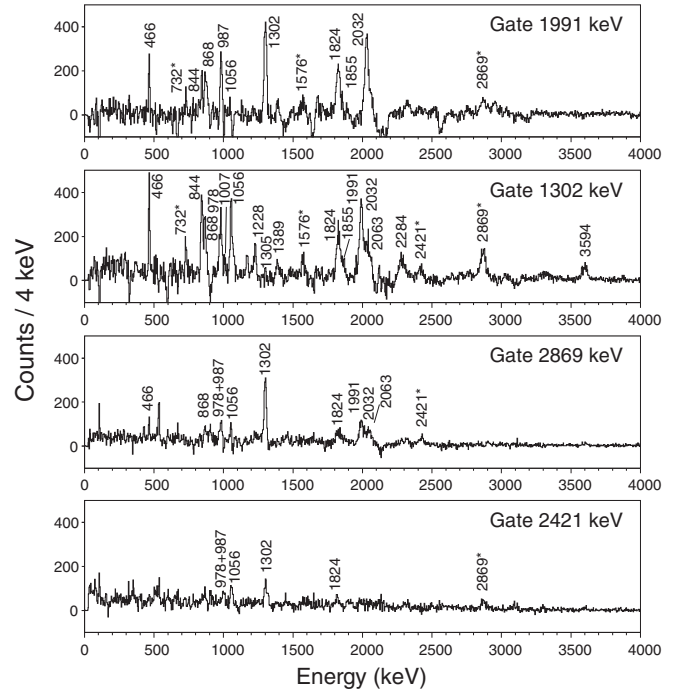


FIG. 1. Background-subtracted γ -ray coincidence spectra gated on the 2α -detected case. New transitions observed in the present paper are marked with an asterisk (*).

and 2869 keV. The spectra gated on 2869- and 2421-keV transitions show that these transitions are mutually in coincidence.

The proposed level scheme in this paper is shown in Fig. 2. New transitions at 732, 1576, 2421, and 2869 keV are

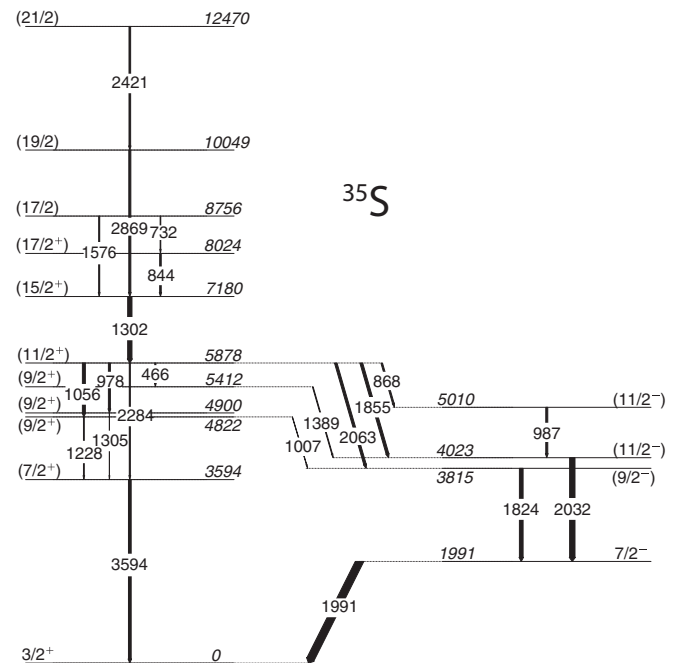


FIG. 2. Proposed level scheme of ^{35}S as deduced from the present paper. The spin-parity assignments below the level at 8024 keV were referred from the prior work [26].

TABLE I. Excited levels, spin and parity assignments for initial and final states, transition energies, relative intensities, and multiplicities of transitions. New levels obtained in the present paper are marked with an asterisk (*). The multipolarity assignments below the 8024-keV levels were referred from the prior work [26].

E (keV)	J_i^π	J_f^π	E_γ (keV)	I_γ^{rel}	R_{ADO}	Multiplicity
1991	$7/2^-$	$3/2^+$	1990.5(4)	100	1.30(8)	$M2 + E3$
3594	$(7/2^+)$	$3/2^+$	3594.4(11)	35(2)	0.93(20)	$E2$
3815	$(9/2^-)$	$7/2^-$	1824.4(6)	48(2)		$M1$
4023	$(11/2^-)$	$7/2^-$	2032.4(4)	70(16)		$E2$
4822	$(9/2^+)$	$(7/2^+)$	1228.3(6)	11(2)		$M1$
		$(9/2^-)$	1007.2(11)	4(2)	0.87(15)	$E1$
4900	$(9/2^+)$	$(7/2^-)$	1305.3(4)	5(3)		$M1$
5010	$(11/2^-)$	$(11/2^-)$	986.6(3)	26(1)	0.91(13)	$M1$
5412	$(9/2^+)$	$(11/2^-)$	1389.0(8)	9(2)		$E1$
5878	$(11/2^+)$	$(7/2^+)$	2283.5(10)	14(3)		$E2$
		$(9/2^-)$	2063.3(14)	32(6)	0.58(41)	$E1$
		$(11/2^-)$	1854.5(42)	28(14)		$E1$
		$(9/2^+)$	1055.6(4)	39(10)	0.67(18)	$M1$
		$(9/2^+)$	978.4(10)	26(7)		$M1$
		$(11/2^-)$	868.2(4)	20(2)	0.54(21)	$E1$
		$(9/2^+)$	465.5(2)	14(1)	0.67(11)	$M1$
7180	$(15/2^+)$	$(11/2^+)$	1301.6(3)	56(11)	1.40(17)	$E2$
8024	$(17/2^+)$	$(15/2^+)$	8443(6)	20(3)	0.51(8)	$M1$
8756*	$(17/2)$	$(15/2^+)$	1576.3(14) ^a	14(3)		$\Delta J = 1$
		$(17/2^+)$	731.6(15) ^a	8(3)	0.43(9)	$\Delta J = 1$
10049*	$(19/2)$	$(15/2^+)$	2868.7(8)	26(2)	0.98(13)	$\Delta J = 2$
12470*	$(21/2)$	$(19/2)$	2420.6(11)	21(6)	0.50(42)	$\Delta J = 1$

^aTransition energy was determined by the Ge detectors placed at 86° and 94° .

assigned as those from the high-excited states. These transitions are placed above the 7180-keV level since they are observed in coincidence with the transitions below the 7180-keV level. The γ -ray coincidence analysis supports the cascade assignments of 732- and 844-keV transitions, which results in an assignment of the new 1576-keV transition as a crossover. All of other assigned peaks are consistent with the prior work [26]. Note that several known low-excited levels [26] could not be observed in the present paper due to the limited statistics for the transition with small relative intensity. The unobserved level are marked in Table II. Spin assignments were performed by the angular distribution from oriented states (ADO ratio) ratio which is calculated by weighted directional correlations from oriented state (DCO ratio) [37] for all possible combinations of the detector angles. The ratio is expressed as

$$R_{\text{ADO}}^{\gamma_i} = \frac{I^{\gamma_i}(47^\circ \text{ gated by } \gamma_2 \text{ at all})}{I^{\gamma_i}(86^\circ \text{ gated by } \gamma_2 \text{ at all})}, \quad (1)$$

where I^γ denotes the intensity of γ transition. For the present setup, values of $R_{\text{ADO}} \approx 0.8$ and ≈ 1.0 are obtained for dipole transition and quadrupole stretched transition, respectively. The values obtained in this paper are shown as a function of transition energy in Fig. 3. Information on observed transitions is summarized in Table I. All of level energies for known levels and the spin assignments are consistent with the prior work [26].

Among the new transitions, residual Doppler energy shifts [38] were observed for the 732- and 1576-keV γ -ray peaks as shown in Fig. 4. Normally, transitions from low-spin states are sufficiently slow so that the decay occurs mainly outside the target. The Doppler energy shifts can be corrected by using the well-defined velocity distribution determined by the known transitions. However, very short-life transitions which decay inside the target produce small amount of energy shifts compared to the transition energy even after the Doppler correction because of the discrepancy of the velocity of compound nuclei between inside and outside the target. The energies are shifted slightly to higher energy for the forward-detection angle whereas lower for the backward-detection

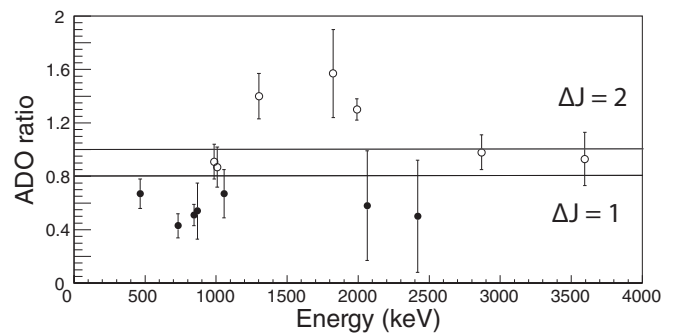


FIG. 3. ADO ratios of the observed transitions in ^{35}S as a function of transition energy. Filled and open circles correspond to assignments for $\Delta J = 1$ and 2, respectively.

TABLE II. Comparison between experimental and calculated levels for ^{35}S . $n\hbar\omega$ represents n -particle n -hole configurations. The values in the column mean the portion of the wave function for each calculated state. The transition probabilities $B(M1)$ and $B(E2)$ were calculated by the shell-model calculations.

Energy (MeV) Experiment	Theory	J_i^π	J_f^π	E_y^{exp} (keV)	Ratio (%)			$B(M1)$ (μ_N^2)	$B(E2)$ ($e^2 \text{fm}^4$)
					$0\hbar\omega$	$2\hbar\omega$	$4\hbar\omega$		
1.572 ^a	1.709	$1/2_1^+$	$3/2_1^+$	1572	57.9	36.9	5.2	0.003	36.3
0.000	0.000	$3/2_1^+$			71.0	26.5	2.4		
2.717 ^a	2.672	$5/2_1^+$	$1/2_1^+$	2717	66.0	30.9	3.2		7.7
3.886 ^a	3.036	$5/2_2^+$			59.9	35.8	4.3		
3.594	3.538	$7/2_1^+$	$3/2_1^+$	3594	50.8	44.1	5.1		28.8
4.822	5.381	$9/2_1^+$	$7/2_1^+$	1228	0.0	86.2	13.8	0.000	5.4
4.900	5.870	$9/2_2^+$	$7/2_1^+$	1305	0.2	85.2	14.6	0.000	0.6
5.412	5.941	$9/2_3^+$	$5/2_2^+$	1526 ^a					11.4
5.878	5.313	$11/2_1^+$	$9/2_1^+$	1056	0.0	86.6	13.4		
		$11/2_2^+$	$9/2_2^+$	978					
		$11/2_3^+$	$9/2_3^+$	466					
6.299	6.776	$11/2_2^+$	$9/2_3^+$	887	0.0	86.3	13.6		4.1
	6.274	$13/2_1^+$			0.0	86.1	13.9		
7.180	6.233	$15/2_1^+$	$11/2_2^+$	1302	0.0	87.0	13.0		51.4
8.024	8.118	$17/2_1^+$	$15/2_1^+$	844	0.0	85.9	14.1	0.001	17.3
	8.736	$17/2_2^+$	$17/2_1^+$	732	0.0	85.9	14.1	0.364	14.7
		$17/2_2^+$	$15/2_1^+$	1576				0.000	27.4
	8.807	$17/2_3^+$	$17/2_1^+$	732	0.0	86.8	13.2	0.046	1.9
		$17/2_3^+$	$15/2_1^+$	1576				0.002	7.2
	9.024	$19/2_1^+$			0.0	88.8	11.2		
	11.181	$21/2_1^+$			0.0	87.5	12.5		
	13.376	$23/2_1^+$			0.0	87.1	12.9		
	15.831	$25/2_1^+$			0.0	12.4	87.6		
					$1\hbar\omega$	$3\hbar\omega$	$5\hbar\omega$		
2.348 ^a	1.837	$3/2_1^-$			72.3	25.6	2.1		
	2.946	$5/2_1^-$			69.5	28.1	2.4		
1.911	1.030	$7/2_1^-$			74.6	23.6	1.8		
3.815	3.166	$9/2_1^-$	$7/2_1^-$	1824	78.1	20.5	1.4	0.013	54.7
4.023	3.356	$11/2_1^-$	$7/2_1^-$	2032	74.6	23.7	1.7		60.9
5.010	4.205	$11/2_2^-$	$7/2_1^-$	987	78.4	20.4	1.3		0.3
		$11/2_2^-$	$11/2_1^-$	3019	78.4	20.4	1.3	0.067	31.1
6.352 ^a	5.637	$13/2_1^-$	$9/2_1^-$	2536 ^a	77.7	21.0	1.4		39.2
		$13/2_1^-$	$11/2_1^-$	2330 ^a				0.017	26.6
	6.239	$15/2_1^-$			74.8	23.5	1.7		
	9.967	$17/2_1^-$			75.4	23.0	1.6		
	10.343	$19/2_1^-$			0.0	93.3	6.7		
	11.366	$21/2_1^-$			0.0	93.8	6.2		
	11.582	$23/2_1^-$			0.0	94.0	6.0		
	13.421	$25/2_1^-$			0.0	93.1	6.9		

^aValues were taken from Ref. [26].

angles than the original transition energy. The existence of the shifts indicates a very short-lived highly excited state. By estimating maximum traveling time of ^{35}S in the thin target, a half-life shorter than 1 ps for the level at 8756 keV is expected.

On the basis of the obtained ADO ratio and the observation of the residual Doppler shifts, we assign $J = (17/2)$ for the level at 8756 keV. As for the high-energy peaks at 2421 and 2869 keV, we assign new levels at 10049 and 12470 keV based on the relative intensities for these transitions. The values of the ADO ratio indicate the dipole and quadrupole natures for the 2421- and 2869-keV transitions, respectively.

As a result, $J = (19/2)$ and $(21/2)$ are assigned for 10049- and 12470-keV level. Note that the ADO ratio indicates only the dipole or quadrupole characters and does not assure the parity assignments. The obtained levels are discussed later with results of the shell-model calculations.

III. SHELL-MODEL CALCULATIONS

A. Level structure in ^{35}S

Large-scale shell-model calculations were performed to interpret the obtained levels. We adopted the SDPF-MSD4

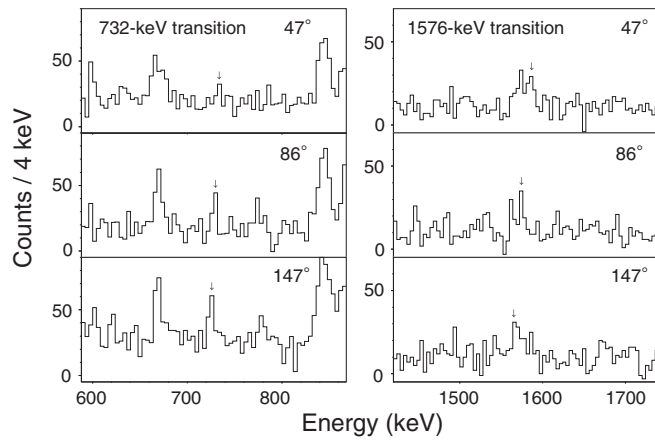


FIG. 4. Residual Doppler shifts for 732- and 1576-keV transitions. The energy shifts are observed in forward (47°), center (86°), and backward angles (147°), respectively.

interaction, which was constructed by modifying the SDPF-M interaction so that the deformed bands of the Ca isotopes and the neighboring nuclei are reproduced well [20]. The model space was taken as the $0d_{5/2}$, $0d_{3/2}$, $1s_{1/2}$, $0f_{7/2}$, and $1p_{3/2}$ single-particle orbits with the ^{16}O inert core. Up to five-particle five-hole excitations were allowed from the filling configuration. The M -scheme dimension reached 1.02×10^9 in the present paper. The calculations were performed with the KSHELL code [39,40]. The comparison between the experimental and the calculated levels up to $J = 17/2$ is shown in Fig. 5.

For yrast states from $J = 1/2$ to $5/2$, positive-parity states could be dominant since the states mainly consist of excitations only within the sd shell. As for the yrast states from $J = 7/2$ to $15/2$, one-particle excitations to the fp shell could be dominant to produce the angular momentum. Two-particle excitations to fp shell could produce the yrast states from $J = 17/2$ to $21/2$. Note that proton excitations over the energy gap at $Z = 20$ are not assumed here.

The excited levels by experimental data and the shell-model calculations as a function of spin are shown in Fig. 6. The levels are colored with red and blue for positive- and negative-parity states, respectively. The positive parity for $1/2$ to $5/2$ and $15/2$ to $21/2$, and the negative-parity states for $7/2$ to $13/2$ are calculated in the yrast levels. The transitioning parity as a function of spin in these yrast levels could be attributed to the number of excited particles to the fp shell.

The details of the obtained levels could be discussed with the dominant configurations for each level. Comparison between experimental and calculated levels is summarized in Table II. The table represents the dominant configuration for each calculated level. For instance, the ground state of ^{35}S is expected to be $J^\pi = 3/2^+$ due to the neutron hole in the $d_{3/2}$ orbital. The $0p$ - $0h$ configuration dominates by 71%. The positive-parity levels below $J^\pi = 7/2^+$ are dominant with the $0p$ - $0h$ configuration whereas the negative-parity states below $J^\pi = 17/2^-$ are dominant with the $1p$ - $1h$ configuration.

The $2p$ - $2h$ configuration takes place above $J^\pi = 9/2^+$, and the dominance appears up to $J = 23/2^+$. The $4p$ - $4h$ config-

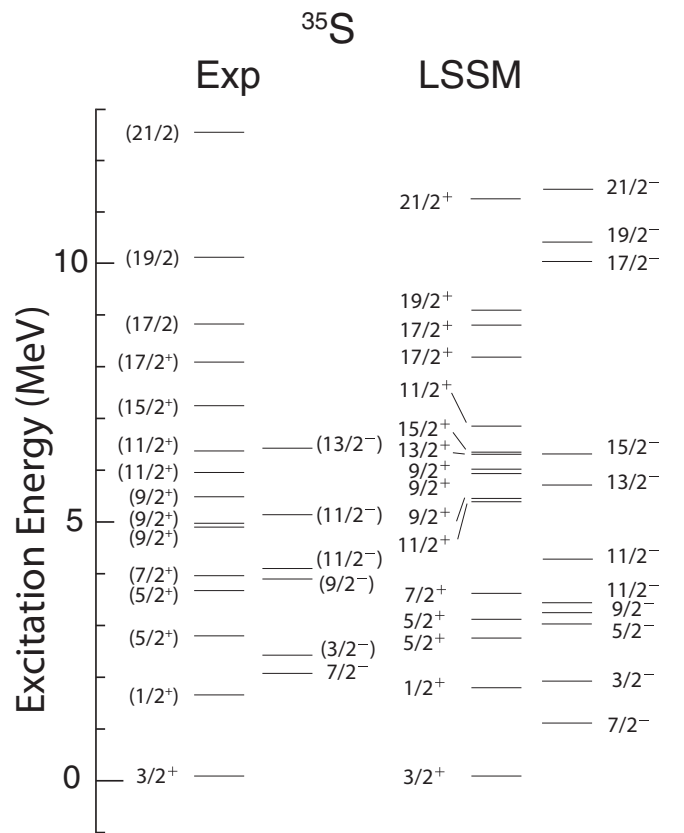


FIG. 5. Experimental levels compared with calculated levels by large-scale shell-model (LSSM) calculations. The experimental levels for low-lying levels were partly taken from Ref. [26].

uration becomes dominant at $J^\pi = 25/2^+$. The significant reduction of $1p$ - $1h$ components is also seen in negative-parity states from $J = 17/2^-$ to $19/2^-$. A recent work by linear polarization measurements on ^{37}Ar [41], which also has 19 neutrons, shows the similar trend for the yrast level structure in $J^\pi = (17/2^+) - (21/2^+)$.

B. pn -pair excited states

Transitions from $(19/2)$ to $(17/2)$ states were not observed experimentally despite the relatively high statistics of the 2869-keV transition from the $(19/2)$ to $(15/2^+)$ states. This fact could be related to different configurations for these high-spin states. In order to understand the origin of the states, limited configuration spaces with one proton-one neutron (pn) or two neutron ($2n$) excitations were applied for the shell-model calculations. The calculated levels with these configurations are shown in Fig. 7. The levels labeled with $2n$ and pn represent the calculated levels which allow only two-neutron, and one-proton-one-neutron excitations, respectively. Positive parities for the $(19/2)$ and $(21/2)$ states are assumed here. Note that the predicted levels for $21/2^+$ and $21/2^-$ are close within 300 keV, therefore, the assignment is still tentative here. One could note that the level energies for $(17/2)$ states obtained in the present paper are close with the calculated results with pn excitations, whereas other levels,

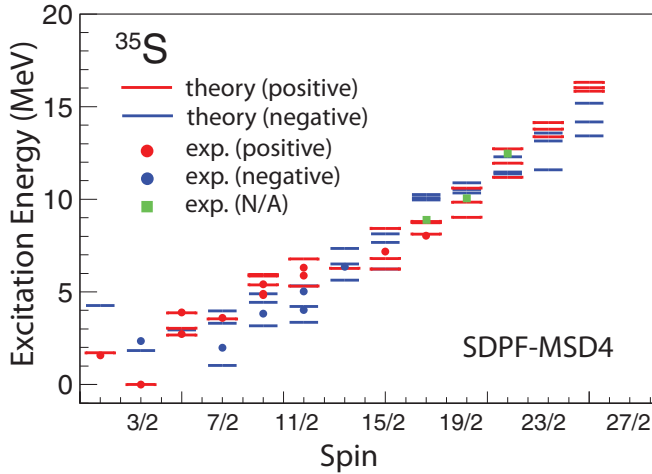


FIG. 6. Excited levels by experimental data and large-scale shell-model calculations as a function of spin. The positive- and negative-parity states are colored with red and blue, respectively. Parities are not available experimentally when the levels are colored with green. Low-excited levels marked with ^a in Table II are taken from prior work [26].

such as (15/2⁺), (19/2), and (21/2) have good agreements with the results of 2*n* excitations.

The transition probabilities could be affected by the difference of the configurations. Here, the parity of 8756 keV was assumed as positive for the following discussion. Note that the parity of the level was not assigned in the present data. The

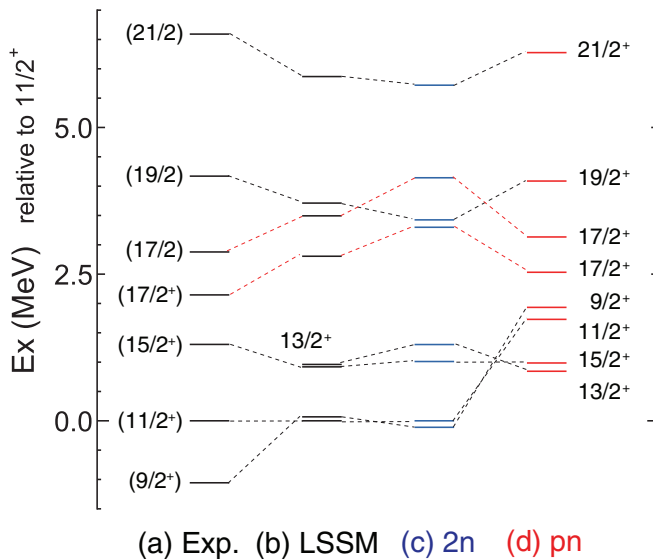


FIG. 7. Comparison between the experimental levels (a: Exp.) and calculated levels (b: LSSM) from the large-scale shell-model calculations relative to 11/2⁺. The 2*n* and *pn* labels represent the calculated levels which allow only two-neutron, and one-proton-one-neutron excitations, respectively. Note that the 17/2⁺ states in the LSSM, 2*n* and *pn* correspond to 17/2_{1,3}⁺ from the shell-model calculations.

experimental branching ratios for 1576- and 732-keV transitions from the level at 8756 keV are 64(18)% and 36(15)%. By using the $B(M1)$, $B(E2)$ values from the shell-model calculations as shown in Table II, the expected branching ratios for the 1576- and 732-keV transitions are calculated to be 59% and 41% when we assume the experimental (17/2₁⁺) at the 8024-keV level and (17/2) at the 8756-keV level to be theoretical 17/2₁⁺ and 17/2₃⁺ levels. These theoretical 17/2₁⁺ and 17/2₃⁺ levels originate from the *pn* excitations to the *fp* shell. On the other hand, the expected branching ratios are calculated to be 12% and 88% if we assume the experimental (17/2) levels to be theoretical 17/2₁⁺ and 17/2₂⁺ levels. The theoretical 17/2₂⁺ level originates from the 2*n* excitations to the *fp* shell. These branching ratios have considerable discrepancies compared to the experimental branching ratios. The dominance of the *pn* excitations to the *fp* shell might be attributed to the $(\pi 0f_{7/2} \times \nu 0f_{7/2})^{(7^+)}\pi 1d_{3/2}$ aligned configuration. The *pn* excitations play important role to interpret the (7⁺) level at 9912 keV in ³⁴S [12]. Since the statistical errors for the branching ratios are still large and the spin-parity assignments for these states were not firmly established, future investigations on high-spin states would provide more quantitative discussion for the *pn*-pair excited states.

IV. SUMMARY

High-spin states of ³⁵S have been studied by the fusion-evaporation reaction of ²⁶Mg(¹⁸O, 2 α 1*n*)³⁵S. The level scheme of ³⁵S was extended up to 12.47 MeV with the γ - γ coincidence analysis and the ADO ratios. The large-scale shell-model calculations were performed with the SDPF-MSD4 interaction. All of the observed levels up to $J = (21/2)$ are explained well within the 2*p*-2*h* excitations from the *sd* to the *fp* shells. The possibility of the *pn*-pair excitation for $J = (17/2)$ states was discussed with the experimental and theoretical results.

ACKNOWLEDGMENTS

We are thankful to the technical staffs of IPN for their support, especially S. Ancelin for supporting us in the construction of the experimental setup, and A. Durnez and V. Petitbon for the fabrication of the ²⁶Mg targets. We also would like to thank the technical staff members of the JAEA tandem accelerator to determine the incident beam energy for the experiment. This work was supported by JSPS-CNRS Bilateral Program, the JSPS/CNRS Joint Research Project, and the French-UK IN2P3-STFC Loan Pool collaboration for the loan of EUROGAM-1 detectors. N.S. and Y.U. acknowledge support by the post-K priority issue 9 (Grants No. hp180179 and No. hp190160), the Program for Promoting Researches on the Supercomputer Fugaku (Grant No. hp200130), and the RCNP Collaboration Research network (Grant No. COREnet). The shell-model calculations were performed mainly on the Oakforest-PACS computer (Grant No. xg18i035).

- [1] A. O. Macchiavelli, P. Fallon, R. M. Clark, M. Cromaz, M. A. Deleplanque, R. M. Diamond, G. J. Lane, I. Y. Lee, F. S. Stephens, C. E. Svensson, K. Vetter, and D. Ward, *Phys. Rev. C* **61**, 041303(R) (2000).
- [2] A. V. Afanasjev and S. Frauendorf, *Phys. Rev. C* **71**, 064318 (2005).
- [3] J. Engel, K. Langanke, and P. Vogel, *Phys. Lett. B* **389**, 211 (1996).
- [4] A. L. Goodman, *Phys. Rev. C* **60**, 014311 (1999).
- [5] W. Satuła and R. Wyss, *Phys. Lett. B* **393**, 1 (1997).
- [6] B. Cederwall, F. Ghazi Moradi, T. Bäck, A. Johnson, J. Blomqvist, E. Clément, G. de France, R. Wadsworth, K. Andgren, K. Lagergren, A. Dijon, G. Jaworski, R. Liotta, C. Qi, B. M. Nyakó, J. Nyberg, M. Palacz, H. Al-Azri, A. Algora, G. de Angelis, A. Ataç, S. Bhattacharyya, T. Brock, J. R. Brown, P. Davies, A. Di Nitto, Zs. Dombrádi, A. Gadea, J. Gál, B. Hadinia, F. Johnston-Theasby, P. Joshi, K. Juhász, R. Julin, A. Jungclaus, G. Kalinka, S. O. Kara, A. Khaplanov, J. Kownacki, G. La Rana, S. M. Lenzi, J. Molnár, R. Moro, D. R. Napoli, B. S. Nara Singh, A. Persson, F. Recchia, M. Sandzelius, J.-N. Scheurer, G. Sletten, D. Soehler, P.-A. Söderström, M. J. Taylor, J. Timár, J. J. Valiente-Dobón, E. Vardaci, and S. Williams, *Nature (London)* **469**, 68 (2011).
- [7] B. Cederwall, X. Liu, Ö. Aktas, A. Ertoprak, W. Zhang, C. Qi, E. Clément, G. de France, D. Ralet, A. Gadea, A. Goasduff, G. Jaworski, I. Kuti, B. M. Nyakó, J. Nyberg, M. Palacz, R. Wadsworth, J. J. Valiente-Dobón, H. Al-Azri, A. Ataç Nyberg, T. Bäck, G. de Angelis, M. Doncel, J. Dudouet, A. Gottardo, M. Jurado, J. Ljungvall, D. Mengoni, D. R. Napoli, C. M. Petrache, D. Soehler, J. Timár, D. Barrientos, P. Bednarczyk, G. Benzoni, B. Birkenbach, A. J. Boston, H. C. Boston, I. Burrows, L. Charles, M. Ciemala, F. C. L. Crespi, D. M. Cullen, P. Désesquelles, C. Domingo-Pardo, J. Eberth, N. Erduran, S. Ertürk, V. González, J. Goupil, H. Hess, T. Huyuk, A. Jungclaus, W. Korten, A. Lemasson, S. Leoni, A. Maj, R. Menegazzo, B. Million, R. M. Perez-Vidal, Zs. Podolyak, A. Pullia, F. Recchia, P. Reiter, F. Saillant, M. D. Salsac, E. Sanchis, J. Simpson, O. Stezowski, C. Theisen, M. Zielińska, *Phys. Rev. Lett.* **124**, 062501 (2020).
- [8] B. S. Nara Singh, Z. Liu, R. Wadsworth, H. Grawe, T. S. Brock, P. Boutachkov, N. Braun, A. Blazhev, A. M. Górska, S. Pietri, D. Rudolph, C. Domingo-Pardo, S. J. Steer, A. Ataç, L. Bettermann, L. Cáceres, K. Eppinger, T. Engert, T. Faestermann, F. Farinon, F. Finke, K. Geibel, J. Gerl, R. Gernhäuser, N. Goel, A. Gottardo, J. Grębosz, C. Hinke, R. Hoischen, G. Ilie, H. Iwasaki, J. Jolie, A. Kaşkaş, I. Kojouharov, R. Krücken, N. Kurz, E. Merchán, C. Nociforo, J. Nyberg, M. Pfützner, A. Prochazka, Zs. Podolyák, P. H. Regan, P. Reiter, S. Rinta-Antila, C. Scholl, H. Schaffner, P.-A. Söderström, N. Warr, H. Weick, H.-J. Wollersheim, P. J. Woods, F. Nowacki, and K. Sieja, *Phys. Rev. Lett.* **107**, 172502 (2011).
- [9] A. Poves and G. Martínez-Pinedo, *Phys. Lett. B* **430**, 203 (1998).
- [10] W. Satuła, R. Wyss, *Nucl. Phys. A* **676**, 120 (2000).
- [11] K. Kaneko, Y. Sun, and G. de Angelis, *Nucl. Phys. A* **957**, 144 (2017).
- [12] P. Mason, N. Märginean, S. M. Lenzi, M. Ionescu-Bujor, F. Della Vedova, D. R. Napoli, T. Otsuka, Y. Utsuno, F. Nowacki, M. Axioti, D. Bazzacco, P. G. Bizzeti, A. Bizzeti-Sona, F. Brandolini, M. Cardona, G. de Angelis, E. Farnea, A. Gadea, D. Hojman, A. Iordachescu, C. Kalfas, T. Kröll, S. Lunardi, T. Martínez, C. M. Petrache, B. Quintana, R. V. Ribas, C. Rossi Alvarez, C. A. Ur, R. Vlastou, and S. Zilio, *Phys. Rev. C* **71**, 014316 (2005).
- [13] C. E. Svensson, A. O. Macchiavelli, A. Juodagalvis, A. Poves, I. Ragnarsson, S. Åberg, D. E. Appelbe, R. A. E. Austin, C. Baktash, G. C. Ball, M. P. Carpenter, E. Caurier, R. M. Clark, M. Cromaz, M. A. Deleplanque, R. M. Diamond, P. Fallon, M. Furlotti, A. Galindo-Uribarri, R. V.F. Janssens, G. J. Lane, I. Y. Lee, M. Lipoglavsek, F. Nowacki, S. D. Paul, D. C. Radford, D. G. Sarantites, D. Seweryniak, F. S. Stephens, V. Tomov, K. Vetter, D. Ward, and C. H. Yu, *Phys. Rev. Lett.* **85**, 2693 (2000).
- [14] E. Ideguchi, S. Ota, T. Morikawa, M. Oshima, M. Koizumi, Y. Toh, A. Kimura, H. Harada, K. Furutaka, S. Nakamura, F. Kitatani, Y. Hatsukawa, T. Shizuma, M. Sugawara, H. Miyatake, Y. X. Watanabe, Y. Hirayama, and M. Oi, *Phys. Lett. B* **686**, 18 (2010).
- [15] E. Ideguchi, D. G. Sarantites, W. Reviol, A. V. Afanasjev, M. Devlin, C. Baktash, R. V. F. Janssens, D. Rudolph, A. Axelsson, M. P. Carpenter, A. Galindo-Uribarri, D. R. LaFosse, T. Lauritsen, F. Lerma, C. J. Lister, P. Reiter, D. Seweryniak, M. Weiszflog, and J. N. Wilson, *Phys. Rev. Lett.* **87**, 222501 (2001).
- [16] A. Bisoi, M. S. Saha, S. Sarkar, S. Ray, M. R. Basu, D. Kanjilal, S. Nag, K. Selvakumar, A. Goswami, N. Madhavan, S. Muralithar, and R. K. Bhowmik, *Phys. Rev. C* **88**, 034303 (2013).
- [17] Y. Taniguchi, *Phys. Rev. C* **99**, 064309 (2019).
- [18] B. A. Brown and B. H. Wildenthal, *Ann. Rev. Nucl. Part. Sci.* **38**, 29 (1988).
- [19] E. K. Warburton, J. A. Becker, and B. A. Brown, *Phys. Rev. C* **41**, 1147 (1990).
- [20] Y. Utsuno, Y. Ichikawa, N. Shimizu, and T. Otsuka (unpublished).
- [21] Y. Utsuno, T. Otsuka, T. Mizusaki, and M. Honma, *Phys. Rev. C* **60**, 054315 (1999).
- [22] E. Caurier, K. Langanke, G. Martínez-Pinedo, F. Nowacki, and P. Vogel, *Phys. Lett. B* **522**, 240 (2001).
- [23] M. Bouhelal, F. Haas, E. Caurier, F. Nowacki, and A. Bouldjedri, *Nucl. Phys. A* **864**, 113 (2011).
- [24] A. Bisoi, A. Das, M. S. Sarkar, and S. Sarkar, *Phys. Rev. C* **97**, 044317 (2018).
- [25] S. Aydin, M. Ionescu-Bujor, G. T. Gavrilo, B. I. Dimitrov, S. M. Lenzi, F. Recchia, D. Tonev, M. Bouhelal, F. Kavillioglu, P. Pavlov, D. Bazzacco, P. G. Bizzeti, A. M. Bizzeti-Sona, G. de Angelis, I. Deloncle, E. Farnea, A. Gadea, A. Gottardo, N. Goutev, F. Haas, T. Huyuk, H. Laftchiev, S. Lunardi, Tz. K. Marinov, D. Mengoni, R. Menegazzo, C. Michelagnoli, D. R. Napoli, P. Petkov, E. Sahin, P. P. Singh, E. A. Stefanova, C. A. Ur, J. J. Valiente-Dobón, and M. S. Yavahchova, *Phys. Rev. C* **96**, 024315 (2017).
- [26] S. Aydin, M. Ionescu-Bujor, F. Recchia, S. M. Lenzi, M. Bouhelal, D. Bazzacco, P. G. Bizzeti, A. M. Bizzeti-Sona, G. de Angelis, I. Deloncle, E. Farnea, A. Gadea, A. Gottardo, F. Haas, T. Huyuk, H. Laftchiev, S. Lunardi, D. Mengoni, R. Menegazzo, C. Michelagnoli, D. R. Napoli, A. Poves, E. Sahin, P. P. Singh, D. Tonev, C. A. Ur, and J. J. Valiente-Dobón, *Phys. Rev. C* **89**, 014310 (2014).
- [27] E. K. Warburton, D. E. Alburger, J. A. Becker, B. A. Brown, and S. Raman, *Phys. Rev. C* **34**, 1031 (1986).
- [28] S. Raman, R. F. Carlton, J. C. Wells, E. T. Journey, and J. E. Lynn, *Phys. Rev. C* **32**, 18 (1985).

- [29] R. M. Freeman, R. Faerber, M. Toulemonde, and A. Gallmann, *Nucl. Phys. A* **197**, 529 (1972).
- [30] A. Guichard, H. Nann, and B. H. Wildenthal, *Phys. Rev. C* **12**, 1109 (1975).
- [31] T. W. van der Mark and L. K. Ter Veld, *Nucl. Phys. A* **181**, 196 (1972).
- [32] B. Fornal, R. H. Mayer, I. G. Bearden, P. Benet, R. Broda, P. J. Daly, Z. W. Grabowski, I. Ahmad, M. P. Carpenter, P. B. Fernandez, R. V. F. Janssens, T. L. Khoo, T. Lauritsen, E. F. Moore, and M. Drigert, *Phys. Rev. C* **49**, 2413 (1994).
- [33] K. Furuno, M. Oshima, T. Komatsubara, K. Furutaka, T. Hayakawa, M. Kidera, Y. Hatsukawa, M. Matsuda, S. Mitarai, T. Shizuma, T. Saitoh, N. Hashimoto, H. Kusakari, M. Sugawara, and T. Morikawa, *Nucl. Instrum. Methods Phys. Res., Sect. A* **421**, 211 (1999).
- [34] S. Go, E. Ideguchi, R. Yokoyama, M. Kobayashi, K. Kismori, S. Michimasa, S. Shimoura, M. Sugawara, M. Koizumi, Y. Toh, T. Shizuma, A. Kimura, H. Harada, K. Furutaka, S. Nakamura, F. Kitatani, and Y. Hatsukawa, *JAEA-Tokai Tandem Ann. Rep.* 2012 13 (2013).
- [35] C. W. Beausang, S. A. Forbes, P. Fallon, P. J. Nolan, P. J. Twin, J. N. Mo, J. C. Lisle, M. A. Bentley, J. Simpson, F. A. Beck, D. Curien, G. deFrance, G. Duchêne, and D. Popescu, *Nucl. Instrum. Methods Phys. Res., Sect. A* **313**, 37 (1992).
- [36] T. Kuroyanagi, S. Mitarai, S. Suematsu, B. J. Min, H. Tomura, J. Mukai, T. Maeda, R. Nakatani, G. Sletten, J. Nyberg, and D. Jerrestam, *Nucl. Instrum. Methods Phys. Res., Sect. A* **316**, 289 (1992).
- [37] A. Krämer-Flecken, T. Morek, R. M. Lieder, W. Gast, G. Hebbinghaus, H. M. Jäger, and W. Urban, *Nucl. Instrum. Methods Phys. Res., Sect. A* **275**, 333 (1989).
- [38] B. Cederwall, I. Y. Lee, S. Asztalos, M. J. Brinkman, J. A. Becker, R. M. Clark, M. A. Deleplanque, R. M. Diamond, P. Fallon, L. P. Farris, E. A. Henry, J. R. Hughes, A. O. Macchiavelli, and F. S. Stephens, *Nucl. Instrum. Methods Phys. Res., Sect. A* **354**, 591 (1995).
- [39] N. Shimizu, T. Mizusaki, Y. Utsuno, and Y. Tsunoda, *Comp. Phys. Commun.* **244**, 372 (2013).
- [40] N. Shimizu, *arXiv:1310.5431*.
- [41] A. Das, A. Bisoi, M. S. Sarkar, S. Sarkar, S. Ray, D. Pramanik, R. Kshetri, S. Nag, P. Singh, K. Selvakumar, A. Goswami, S. Saha, J. Sethi, T. Trivedi, B. S. Naidu, R. Donthi, V. Nanal, and R. Palit, *Phys. Rev. C* **101**, 044310 (2020).